



# Young brown dwarfs: IMF, disks, spatial distribution, and binarity

K. L. Luhman, G. Fazio, T. Megeath, L. Hartmann, and N. Calvet

Smithsonian Astrophysical Observatory, 60 Garden Street, Cambridge, MA 02138, USA

## Abstract.

We present new results regarding the initial mass function, circumstellar disks, spatial distribution, and binarity of young brown dwarfs.

**Key words.** infrared: stars — stars: evolution — stars: formation — stars: low-mass, brown dwarfs — stars: pre-main sequence

## 1. Definition of Young Brown Dwarfs

We first describe the definition of a brown dwarf used in this discussion. The evolutionary models of Baraffe et al. (1998) and Chabrier et al. (2000) provide the best agreement with the available observations tests (Luhman et al. 2003b), such as dynamical mass estimates for young stars and empirical isochrones defined by young multiple systems. If we combine these models with a compatible temperature scale (Luhman et al. 2003b), then the hydrogen burning limit at ages of a few million years is near a spectral type of M6. Note that many of the objects that are referred to as young brown dwarfs in the literature have spectral types earlier than M6 and therefore are more likely to be low-mass stars than brown dwarfs. In addition, the spectral types reported for young late-type objects can be subject to systematic errors, such as those measured from near-IR steam absorption bands. At a given optical spectral type, these bands are stronger in young objects than in field dwarfs (Luhman & Rieke 1999; Lucas et al. 2001; McGovern et al. 2004). As a result, if a young source is classified by compar-

ing the strength of its steam absorption to that of field dwarfs, the derived spectral type will be systematically too late. To arrive at accurate spectral types, optically-classified young objects rather than dwarfs should be used as the standards (Luhman & Rieke 1999; Luhman et al. 2003b).

## 2. IMF of Brown Dwarfs

Recent spectroscopic surveys of Taurus (Luhman 2000; Briceño et al. 2002; Luhman et al. 2003a; Luhman 2004c) and IC 348 (Luhman et al. 2003b) have reported brown dwarf fractions that are a factor of two lower than the values derived from luminosity function modeling in the Trapezium Cluster in Orion (Luhman et al. 2000; Hillenbrand & Carpenter 2000; Muench et al. 2002). The IMFs for these regions are shown in Figure 1. However, upon spectroscopy of a large sample of brown dwarf candidates in the Trapezium, Slesnick et al. (2004) found a population of faint objects with stellar masses, possibly seen in scattered light, which had contaminated previous photometric IMF samples and re-

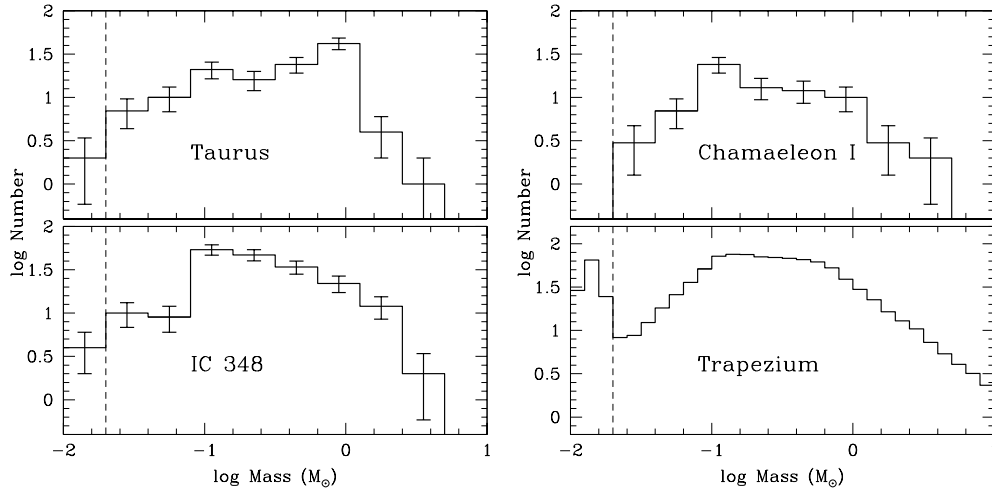


**Fig. 1.** IMFs for Taurus (Luhman 2004c), IC 348 (Luhman et al. 2003b), Chamaeleon I (K. L. Luhman, in preparation), and the Trapezium Cluster (Muench et al. 2002). In the units of this diagram, the Salpeter slope is 1.35.

sulted in overestimates of the brown dwarf fraction in this cluster. After they corrected for this contamination, the brown dwarf fraction in the Trapezium was a factor of  $\sim 1.8$  higher than the value in Taurus from Luhman et al. (2003a). This difference is reduced further ( $\sim 1.4$ ) if the new brown dwarf fraction for Taurus from Luhman (2004c) is adopted. In summary, according to the best available data, the brown dwarf fractions in Taurus and IC 348 are lower than in the Trapezium, but by a factor (1.4-1.8) that is smaller than that reported in earlier studies.

### 3. Brown Dwarf Disks

The first detections of IR excess emission from young brown dwarfs were presented by Comerón et al. (1998) and Luhman (1999). At that time, motivated by these results, the Spitzer IRAC GTO team designed deep imaging of nearby star-forming regions to study disks around brown dwarfs, with a particular emphasis on the regions considered in deep spectroscopic surveys for young brown dwarfs (Luhman 1999). Figure 2 shows a color-color diagram consisting of  $m(5.8 \mu\text{m})-m(8.0 \mu\text{m})$  versus  $m(3.6 \mu\text{m})-m(4.5 \mu\text{m})$  from

IRAC on Spitzer. The circles and points are the predicted colors from models of Class I (star+disk+envelope) and Class II (star+disk) sources, respectively. Class III (naked star) sources have neutral colors and appear near the origin in the color-color diagrams. We adopt the solid lines to separate these classes. In comparison, in Figure 2 we present measurements of  $m(5.8 \mu\text{m})-m(8.0 \mu\text{m})$  versus  $m(3.6 \mu\text{m})-m(4.5 \mu\text{m})$  for a sample of known young stars and brown dwarfs in Taurus. The objects with mid-IR excesses (Class I and II) are easily identified in these data.

Although photometry can be obtained with ground-based facilities for brighter brown dwarfs at the shorter mid-IR bands if the exact location of the brown dwarf is known, ground-based instruments are not capable of performing wide-field searches for new faint mid-IR sources, such as Class I brown dwarfs. In comparison, with its wide field of view and high sensitivity, Spitzer is ideally suited for work of this kind. Using a diagram like Figure 2 for IC 348, we have identified several new objects that have not been previously confirmed as members or field stars and that exhibit colors indicative of Class I sources. We investigate the masses of these Class I candidates

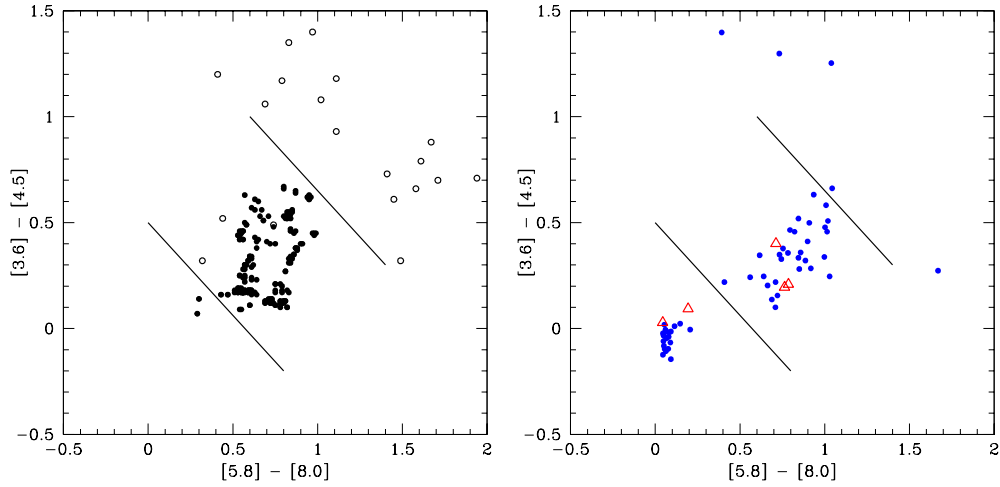


**Fig. 2.** Left: Predicted Spitzer IRAC  $[5.8] - [8.0]$  versus  $[3.6] - [4.5]$  from models of Class I (circles) and Class II (points) sources. Class III sources appear near the origin. The solid lines were selected to mark the boundaries between these classes. Right: Members of the Taurus star-forming region with spectral types of  $\leq M6$  (points) and  $> M6$  (triangles), which correspond to stars and brown dwarfs according to the evolutionary models of Baraffe et al. (1998).

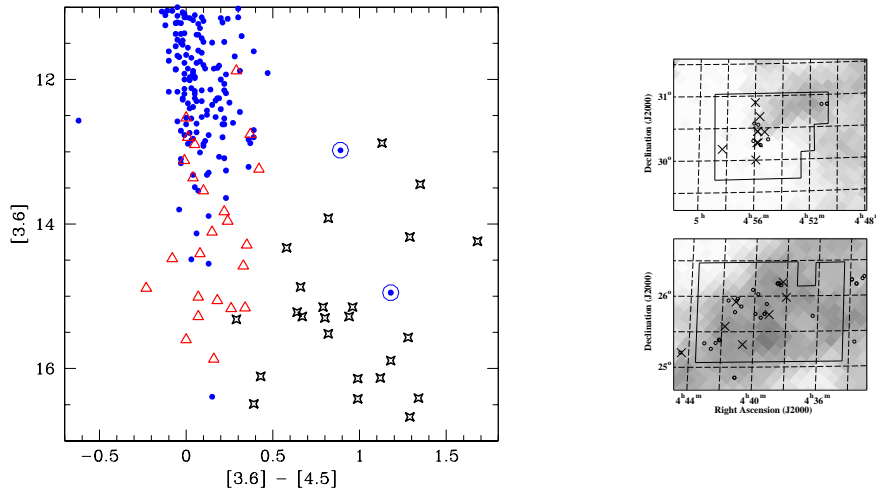


**Fig. 3.** Left: Spitzer IRAC  $[3.6] - [4.5]$  versus  $[3.6]$  for members of IC 348 with spectral types of  $\leq M6$  (points) and  $> M6$  (triangles) and for candidate Class I sources from a diagram like those in Figure 2 (stars). Class I objects among the known members are indicated (circles), the fainter of which is near the hydrogen burning limit according to its M6 spectral type. Right: Spatial distribution of previously known, high-mass members of the Taurus star-forming region (circles) and new, low-mass members from Luhman (2004c) (crosses) shown with emission in  $^{12}\text{CO}$  (grayscale, T. Megeath, private communication). The regions surveyed by Luhman (2004c) are indicated by the solid boundaries.

by plotting them on the color-magnitude diagram in Figure 3 along with the known stellar and substellar members of IC 348. Among the known members, there are two Class I objects, whose spectral types imply masses of  $\sim 0.4$  and  $0.09 M_{\odot}$ . The latter source, which is near the hydrogen burning mass limit, is the least massive known Class I object. In comparison to this source, most of the new candidate Class I objects are even fainter in Figure 3. Therefore, these data may represent the first detections of Class I brown dwarfs, or protobrown dwarfs. However, it is also possible that these candidates have stellar masses. Because Class I sources are often seen only in scattered light, their apparent brightnesses are not reliable indicators of mass. For instance, the nominal magnitude of a cluster member at a mass of  $0.09 M_{\odot}$  in Figure 3 is near  $m(3.6 \mu\text{m}) \sim 12$ , and yet the known Class I source at  $0.09 M_{\odot}$  appears much fainter, probably because it is observed only in scattered light. As a result, the new candidate Class I sources could have similar masses as the brighter, known Class I stars, but appear fainter because the efficiency of their scattering is lower. To better constrain their masses, measurements of spectral types for these candidate Class I brown dwarfs are required. Regardless of the masses of these particular candidates, these observations demonstrate the unique capability of IRAC on Spitzer to efficiently detect sources at the magnitudes and colors expected for protobrown dwarfs.

#### 4. Spatial Distribution of Young Brown Dwarfs

Reipurth & Clarke (2001), Boss (2001), and Bate et al. (2002) have suggested that brown dwarfs could form as protostellar sources whose accretion is prematurely halted by ejection from multiple systems. The resulting spatial distributions of the ejected brown dwarfs might differ from those of the stellar members. Alternatively, if brown dwarfs and stars form in the same manner, then they should exhibit similar spatial distributions. Kroupa & Bouvier (2003a) and Kroupa & Bouvier (2003b) have investigated these scenarios in

detail through dynamical modeling of Taurus-like aggregates of stars and brown dwarfs. In the model in which stars and brown dwarfs form in the same manner, they found that most of the brown dwarfs indeed shared the same spatial distributions as the stars and a high binary fraction, while a small tail of higher velocity ( $v > 1 \text{ km s}^{-1}$ ) brown dwarfs were distributed more widely than the stars and were predominantly single. In comparison, the ejection model also produces widely distributed single brown dwarfs, but they are the dominant population among the brown dwarfs and thus exhibit a shallow density distribution (Kroupa & Bouvier 2003a). Based on their interpretation of measurements of the IMF in Taurus, the Trapezium, and the field, Kroupa & Bouvier (2003b) tended to favor the ejection model. However, Briceño et al. (2002) found no statistically significant differences in the distribution of the high- and low-mass members of Taurus. Similarly, we find that the spatial distribution of the newest low-mass members from Luhman (2004c) closely matches that of the previously known, more massive young stars, as demonstrated in Figure 3. Thus, the available data are better reproduced by the model in which stars and brown dwarfs have a common formation mechanism (Kroupa & Bouvier 2003a) than the ejection model (Kroupa & Bouvier 2003b).

#### 5. Brown Dwarf Binarity

Models for the origin of brown dwarfs can be tested through measurements of the multiplicity of substellar objects. Significant progress in this area has been made through extensive direct imaging of primaries in the field with masses near and below the hydrogen burning mass limit (Burgasser et al. 2003). In the data from these surveys, binary brown dwarfs occur at a rate of  $\sim 15\%$  for separations of  $a > 1 \text{ AU}$  and exhibit maximum separations of  $a \sim 20 \text{ AU}$ . Ejection models predict a somewhat lower binary fraction ( $\sim 5\%$ ) but a similar maximum separation ( $a \sim 10 \text{ AU}$ ) (Bate et al. 2002). Burgasser et al. (2003) concluded that the observed maximum separation

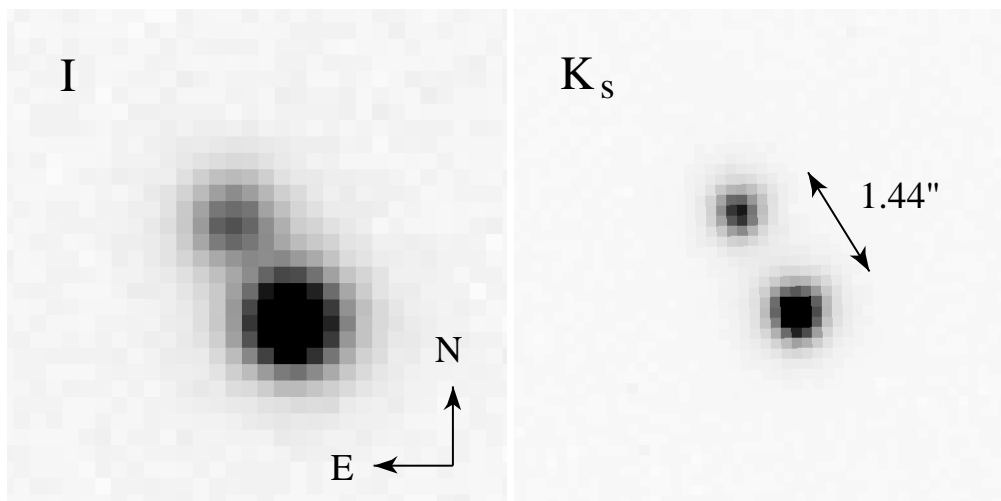


**Fig. 4.** Images of the binary system 2M 1101-7732AB at  $I$  and  $K_s$  (FWHM=  $0''.85$  and  $0''.39$ ).

is not a reflection of disruption of wider binaries by interactions with stars or molecular clouds, which is supported by the absence of wide binaries among substellar primaries in less evolved populations in open clusters (Martín et al. 2003) and in star-forming regions (Neuhäuser et al. 2002; Bouy et al. 2004). Instead, Burgasser et al. (2003) suggested that wide low-mass binaries do not form or are disrupted at a very early stage.

In Luhman (2004b), we recently presented observations of a new faint double, 2MASS J11011926-7732383AB, toward the Chamaeleon I star-forming region. From the optical and near-infrared images of the pair in Figure 4, we measured a separation of  $1''.44$  and extract  $R I J H K_s$  photometry of the components ( $I_A = 17.21$ ,  $\Delta I = 1.07$ ,  $K_{sA} = 11.97$ ,  $\Delta K_s = 0.84$ ). We used resolved optical spectroscopy to derive spectral types of M7.25 and M8.25 for the A and B components, respectively. Based on the strengths of gravity-sensitive features in these data, such as the Na I and K I absorption lines, we concluded that these objects are young members of Chamaeleon I rather than field stars. The probability that this pair is composed of unrelated late-type members of Chamaeleon I is low enough ( $\sim 5 \times 10^{-5}$ ) to definitively establish it as a binary system. After estimating

extinctions, effective temperatures, and bolometric luminosities for the binary components, we placed them on the H-R diagram and inferred their masses with the evolutionary models of Chabrier and Baraffe, arriving at substellar values of  $0.05$  and  $0.025 M_\odot$ . The projected angular separation of this system corresponds to  $240$  AU at the distance of Chamaeleon I, making it the first known binary brown dwarf with a separation greater than  $20$  AU. This demonstration that brown dwarfs can form in fragile, easily disrupted configurations is direct evidence that the formation of brown dwarfs does not require ejection from multiple systems or other dynamical effects. It remains possible that ejection plays a role in the formation of some brown dwarfs, but it is not an essential component according to these observations. Instead, it appears that brown dwarfs can arise from standard, unperturbed cloud fragmentation.

*Acknowledgements.* This work was supported by grant NAG5-11627 from the NASA Long-Term Space Astrophysics program.

## References

- Baraffe, I., Chabrier, G., Allard, F., & Hauschildt, P. H. 1998, *A&A*, 337, 403

- Bate, M. R., Bonnell, I. A., & Bromm, V. 2002, *MNRAS*, 332, L65
- Boss, A. 2001, *ApJ*, 551, L167
- Bouy, H., et al. 2004, *A&A*, 424, 213
- Briceño, C., Luhman, K. L., Hartmann, L., Stauffer, J. R., & Kirkpatrick, J. D. 2002, *ApJ*, 580, 317
- Burgasser, A. J., Kirkpatrick, J. D., Reid, I. N., Brown, M. E., Miskay, C. L., & Gizis, J. E. 2003, *ApJ*, 586, 512
- Chabrier, G., Baraffe, I., Allard, F., & Hauschildt, P. H. 2000, *ApJ*, 542, 464
- Comerón, F., Rieke, G. H., Claes, P., Torra, J., & Laureijs, R. J. 1998, *A&A*, 335, 522
- Hillenbrand, L. A., & Carpenter, J. M. 2000, *ApJ*, 540, 236
- Kroupa, P., & Bouvier, J. 2003a, *MNRAS*, 346, 343
- Kroupa, P., & Bouvier, J. 2003b, *MNRAS*, 346, 369
- Lucas, P. W., Roche, P. F., Allard, F., & Hauschildt, P. H. 2001, *MNRAS*, 326, 695
- Luhman, K. L. 1999, *ApJ*, 525, 466
- Luhman, K. L. 2000, *ApJ*, 544, 1044
- Luhman, K. L. 2004a, *ApJ*, 602, 816
- Luhman, K. L. 2004b, *ApJ*, 614, 398
- Luhman, K. L. 2004c, *ApJ*, in press
- Luhman, K. L., & Rieke, G. H. 1999, *ApJ*, 525, 440
- Luhman, K. L., et al. 2000, *ApJ*, 540, 1016
- Luhman, K. L., Briceño, C., Stauffer, J. R., Hartmann, L., Barrado y Navascués, D., & Nelson, C. 2003a, *ApJ*, 590, 348
- Luhman, K. L., Stauffer, J. R., Muench, A. A., Rieke, G. H., Lada, E. A., Bouvier, J., & Lada, C. J. 2003b, *ApJ*, 593, 1093
- Martín, E. L., Barrado y Navascués, D., Baraffe, I., Bouy, H., & Dahm, S. 2003, *ApJ*, 594, 525
- McGovern, M. R., Kirkpatrick, J. D., McLean, I. S., Burgasser, A. J., Prato, L., & Lowrance, P. J. 2004, *ApJ*, 600, 1020
- Muench, A. A., Lada, E. A., Lada, C. J., & Alves, J. 2002, *ApJ*, 573, 366
- Muzerolle, J., Luhman, K. L., Briceño, C., Hartmann, L., & Calvet, N. 2004, *ApJ*, in press
- Neuhäuser, R., Guenther, E., Mugrauer, M., Ott, T., & Eckart, A. 2002, *A&A*, 395, 877
- Reipurth, B. & Clarke, C. 2001, *AJ*, 122, 432
- Slesnick, C. L., Hillenbrand, L. A., & Carpenter, J. M. 2004, *ApJ*, 610, 1045